



Natural convection of air between parallel plates under strong magnetic field

メタデータ	言語: eng 出版者: 公開日: 2020-01-31 キーワード (Ja): キーワード (En): 作成者: Kaneda, Masayuki, Suga, Kazuhiko メールアドレス: 所属:
URL	http://hdl.handle.net/10466/00016715

NATURAL CONVECTION OF AIR BETWEEN PARALLEL PLATES UNDER STRONG MAGNETIC FIELD

Masayuki Kaneda[§] and Kazuhiko Suga

Dept. of Mech. Eng., Osaka Prefecture Univ., Sakai, Japan

[§]Correspondence author. Fax: +81 72 2549904 Email: mkaneda@me.osakafu-u.ac.jp

ABSTRACT

The effect of a magnetic field on the natural convection of a paramagnetic fluid is numerically studied between vertical heated parallel plates. The magnetic field is presumed by the Ampere's law from electric wires. The heat and fluid flow is simultaneously solved by the lattice Boltzmann method (LBM). For the evaluation of the natural convection by the LBM, a validation is firstly carried out in a square cavity in the absence of the magnetic field. It is confirmed that single-relaxation-time LBM has a comparable validity to the reference data. For the natural convection between the parallel plates under the magnetic field, the magnetothermal force is induced as a repelling force from the magnet. This is because the hotter fluid receives weaker magnetic force than the fluid at reference temperature. This magnetothermal force locally affects the heat and fluid flow near the walls, resulting in enhancement and suppression of the natural convection. In this study, the effect of the magnetic field by electric wires is investigated for two cases; facing different magnetic poles (N-S) and same poles (N-N). It is found that, when the magnetic field is presumed by electric wires, the magnetothermal force becomes similar in both cases, resulting in the similar effects on the heat and fluid flow. This is because that the force in the vicinity of the wire is dominant on the effects.

KEYWORDS: Natural convection, Paramagnetic fluid, Magnetothermal force, Magnetic field

INTRODUCTION

The magnetic susceptibility is a physical property which represents how a material is affected by a magnetic field. The positive susceptibility means that, the material is attracted to the magnet. The ferromagnetic materials (iron, cobalt, nickel) have large positive magnetic susceptibility. The paramagnetic materials (oxygen, air, etc.) also have positive value, but much smaller value than that of ferromagnetic materials. Although this characteristic was found in the past [1] and applied to the gas sensors, the magnetic force on the paramagnetic material has not been under the spotlight for a long time because the attraction force is not remarkable by using weak permanent magnets.

Since the emergence of superconducting magnet, tesla-order magnetic induction has become available. Various new findings have been reported such as the levitation of a water droplet [2], a nitrogen jet [3], magnetoarchimedes effect [4]. The application of the strong magnetic field has been also discussed on the protein crystallization [5], convection enhancement / suppression in Rayleigh-Benard convection [6], natural convection in a cubic enclosure [7], and inside concentric annuli [8]. The magnetic force was found to be comparative to the natural convection [9].

The convection control by the magnetic field owes another characteristic. The magnetic susceptibility of the paramagnetic materials depends on the inverse of the absolute temperature, which is called Curie's law. In other words, colder paramagnetic materials can be attracted stronger to the magnet than hotter ones. Therefore, this magnetic force is called magnetothermal force.

As reviewed, the effect on the convection was examined to closed system. This is because that the magnetic force can be enhanced when the enclosure is sandwiched by two magnets. Also, the effect can be discussed by comparing with exiting Nusselt-Rayleigh correlations. Therefore, the study on open systems are not found except open-ended pipe [3, 10-14]. In the numerical simulation, magnetic field can be modelled by an electric coil which is concentric to the pipe. Thus the phenomenon can be considered in axisymmetric. For an engineering applications, other open systems should be also

considered such as the natural convection between heated parallel plates because this phenomenon is observed in the fin heat exchanger and its heat transfer characteristic is important.

In this study, therefore, effect of the magnetic field is numerically investigated for air convection between vertical heated parallel plates. In this study, two magnetic fields are employed both are induced by electric wires.

COMPUTATIONAL METHOD

Magneto-thermal Lattice Boltzmann Method The heat and fluid flow is simultaneously solved by the lattice Boltzmann method (LBM). In the present study, two-dimensional nine-discrete velocity (D2Q9) model is employed, which is illustrated in Fig. 1. Two distribution functions are respectively employed for the density f_α and the thermal energy g_α . The time evolution equations of both distribution functions at the lattice site r and time t are as follows in the single-relaxation-time BGK model.

$$f_\alpha(r + e_\alpha \delta t, t + \delta t) = f_\alpha(r, t) - \frac{\delta t}{\tau_f + 0.5\delta t} (f_\alpha(r, t) - f_\alpha^{eq}(r, t)) + \frac{\tau_f}{\tau_f + 0.5\delta t} F_\alpha \quad (1)$$

$$g_\alpha(r + e_\alpha \delta t, t + \delta t) = g_\alpha(r, t) - \frac{\delta t}{\tau_g + 0.5\delta t} (g_\alpha(r, t) - g_\alpha^{eq}(r, t)) \quad (2)$$

The superscript eq represents the equilibrium state. The discrete vector is e_α . τ_f and τ_g are the relaxation times for f_α and g_α , respectively. In the density distribution function (Eq.(1)), external forces due to the buoyancy F_g and magneto-thermal forces F_m are considered. The expression of the external force is referred to He et al. [15].

$$F_\alpha = \frac{(F_g + F_m) \times (e_\alpha - u)}{RT_0} f_\alpha^{eq} \quad (3)$$

Where,

$$F_g = -\beta \rho_0 (T - T_0) g \quad (4)$$

$$F_m = -\frac{\beta \rho_0 \chi_0}{\mu_m} (T - T_0) \nabla \mathbf{b}^2 \quad (5)$$

These suggest followings. The buoyancy force works due to temperature difference modelled by the Boussinesq approximation. The magneto-thermal force depends on the magnetic susceptibility χ , the temperature difference from the reference temperature, and the local gradient of the squared magnetic induction. The derivation of the magneto-thermal force is referred from Kaneda et al. [16].

The macroscopic parameters are related to density distribution functions and relaxation times as follows.

$$\rho = \sum_\alpha f_\alpha, \quad \rho u = \sum_\alpha f_\alpha e_\alpha + 0.5 F_\alpha, \quad p = \frac{1}{3} \rho, \quad \nu = \frac{1}{3} \tau_f, \quad T = \sum_\alpha g_\alpha(r, t), \quad D = \frac{1}{3} \tau_g \quad (6-11)$$

Where, D is the thermal diffusivity.

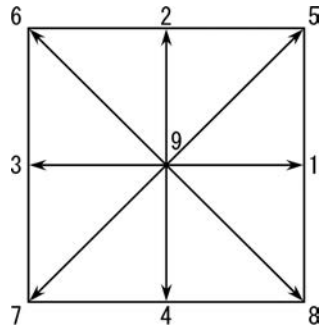


Fig. 1 D2Q9 model.

Evaluation of Lattice Boltzmann Method on Natural Convection in a Square Cavity Firstly, the validation exercise is carried out for the natural convection in a square cavity. In the LBM, the Prandtl number is adjusted by the relaxation times since they are related to the kinematic viscosity and the thermal diffusivity, respectively. In this section, the Prandtl number is presumed to 0.71. The Rayleigh number can be set by giving the corresponding value to the gravity acceleration and volumetric expansion coefficient because the dimensionless temperature is respectively given as boundary conditions on hot and cold walls, and other dimensionless physical properties are fixed due to the relaxation times. The boundary conditions are given by the half-way bounce-back manner. The node number for the fluid domain is 200^2 , which is sufficient for the grid independent result.

The resulted average Nusselt number on the hot wall is listed in Table 1. The results depend on the combination of the relaxation time even though the estimated Prandtl number is identical. After some numerical tests, the appropriate combination of the relaxation times is confirmed, which are $\tau_f=0.08875$ and $\tau_g=0.1250$. For the comparison, well-known benchmarks by Hortmann et al. [17] and de Vahl Davis [18] are referred. It is confirmed that the present scheme has sufficient validation.

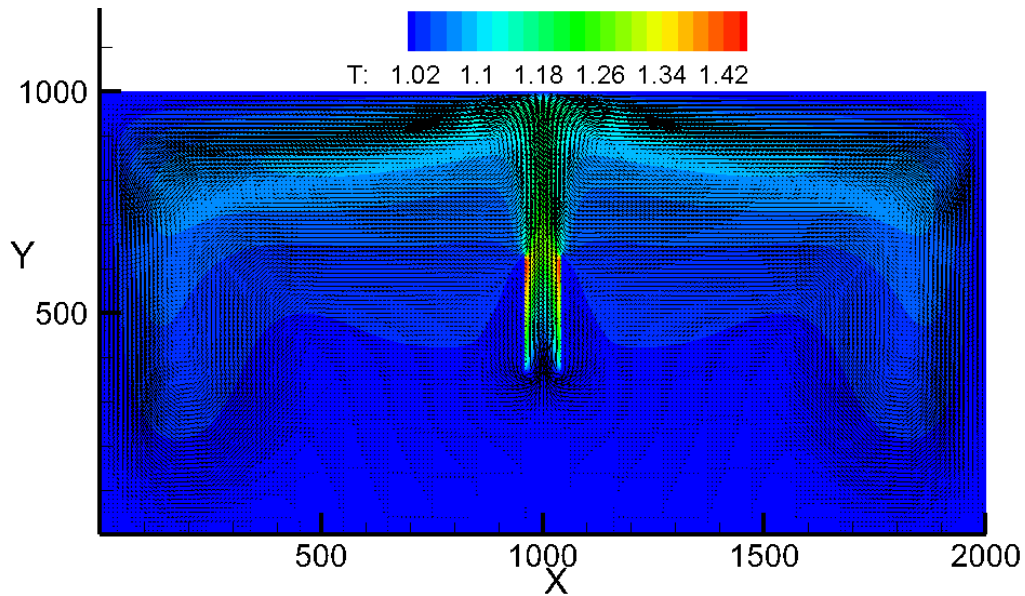
Table 1
Average Nusselt Number on Heated Wall in a Square Cavity

	Rayleigh number		
	10^4	10^5	10^6
Present model	2.245	4.522	8.821
Hortmann et al.	2.245	4.521	8.825
de Vahl Davis	2.238	4.509	8.817

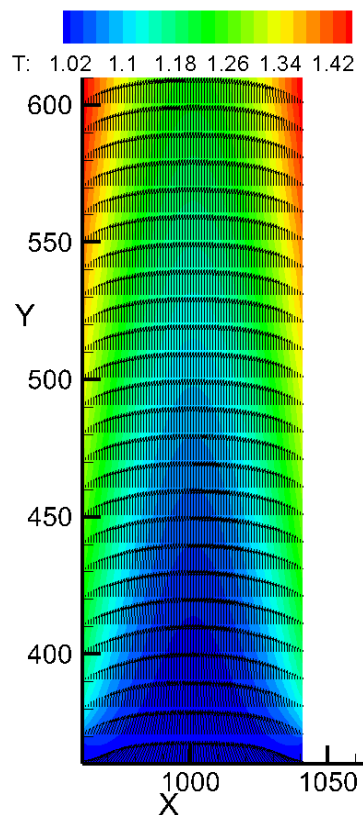
Computational Domain The computational domain is shown in Fig.2. Two vertical heated plates are located at the center of an enclosure. The grid number of the enclosure is 2000×1000 . The length of the heated plate in the enclosure is 262, and the gap of two plates is 82. The enclosure wall is non-slip and kept at a constant temperature ($T=1.0$). Two vertical plates are heated at a constant heat flux. This model, therefore, considers not only the natural convection along the heated plate but also the descending flow along the domain. This is because that, the lattice Boltzmann method has less precision for the free-inlet boundary condition which can be applied at the bottom of the heated walls. To improve the computational speed, the computation is carried out by CUDA fortran up to 5×10^5 timesteps.

The computational grid numbers are decided by the following strategies. First, the buoyant upflow between the plates are not interrupted by the top and bottom walls. Thus the parallel plates are located in the center of the computational domain, and the height of the domain is sufficiently large. Second, the descending flow out of the parallel plates should be far away from the parallel plates. If the width of the domain is small, the descending flow is found to affect the upflow above the parallel plates are affected and the buoyant flow becomes unsteady. By the preliminary test, the grid numbers in the X direction is decided.

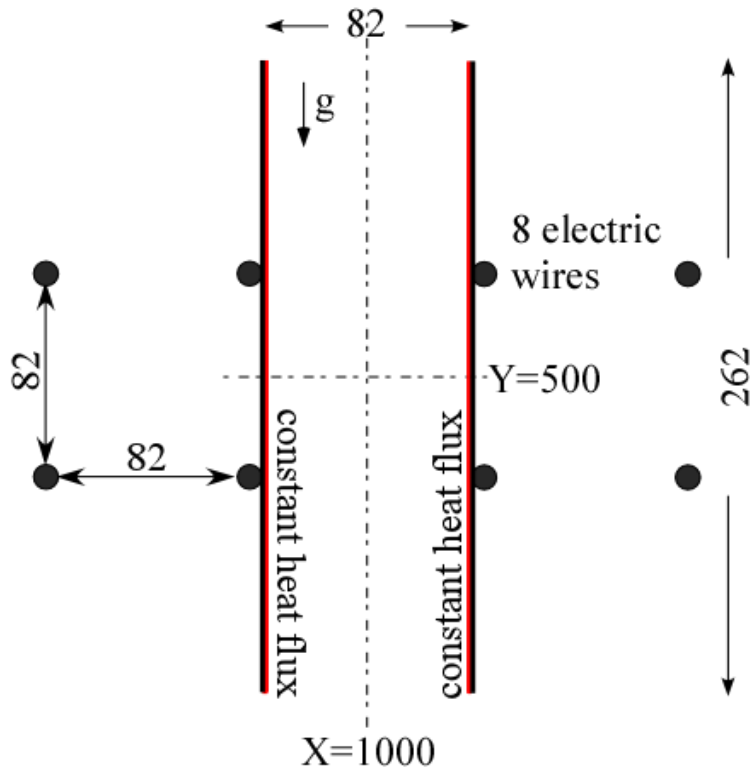
As shown in Fig. 2(a), the buoyancy flow is induced by the heated plates, and the fluid is cooled by the enclosure wall (Note that the number of vector is reduced for a better understanding). Thus the natural convection occurs inside the computational domain. It is confirmed that, a steady-state convection is attained and the heat balance is kept in the enclosure. The natural convection between the parallel plates is also in steady state and reasonable as shown in Fig. (b). Subsequent discussion is imposed on between the parallel plates with magnetic fields. For reference, the schematic drawing is shown in Fig.2(c) with locations of electric wires to induce the magnetic field.



(a) whole computational domain



(b) enlarged image between parallel heated plates



(c) schematic drawing of the heated parallel plates and electric wires

Fig. 2 Induced natural convection in the computational domain without magnetic field. The number in axis corresponds to the node number and length.

Magnetic Field The magnetic field from one virtual magnet is considered by four electric wires located at four edges of the square block magnet whose size is 82×82 nodes. In the present study, a pair of magnets is presumed, thus 8 wires are employed. The induced magnetic field is defined by Ampere's law, and the direction of the magnetic field depends on the direction of the electric current. In the present study, two virtual magnets are employed with two different magnetic field; a cusp-shaped magnetic field by facing same magnetic poles, and a uniform magnetic field facing opposite magnetic poles. Since this study aims to investigate the effect of the magnetothermal force on the natural convection between parallel heated plates, the heat and fluid flow inside the gap of heated plates are imposed.

RESULTS AND DISCUSSION

Computed Magnetic Field and its Gradient The resulted magnetic field and the gradient of squared magnetic induction ∇B^2 are shown in Fig.3 for both magnetic fields. In the cases, four electric wires are placed on the apexes of a square of 80×80 . To avoid the divergence of the magnetic field calculation, offset of wire is 5 nodes from the heated walls. As represented in Eq.(5), ∇B^2 is an important component of the magnetothermal force.

In Fig. 3(a), the uniform magnetic field is attained to some extent. However, even within the magnet-covered area, the magnetic induction has a distribution. This is due to the assumption of the magnetic field by electric wires and leakage of the magnetic field toward another magnetic pole. For the cusp-shape magnetic field (Fig. 3(b)), the magnetic induction is cancelled at mid-centre inbetween magnets, and the magnetic field spreads towards another pole of each magnet.

It is obvious that, the maximum magnetic induction $|B|_{\max}$ is identical due to the same magnitude of the presumed electric current in the wire. In the conventional study using magnetic field, it has been

reported that the cusp-shape magnetic field is more effective than the uniform magnetic field. This is because that, the magnitude of ∇B^2 becomes large for cusp-shape magnetic field by using block magnets or existing electromagnets. However, when the magnetic field is presumed by electric coils, it is found that the profile of ∇B^2 is similar each other. For the maximum value of ∇B^2 , it is interesting that the case of uniform magnetic field has a bit larger than the cusp-shape field at the nearest points to the electric wire.

Magnetothermal force The magnetothermal force is resulted from the temperature and ∇B^2 distributions as Eq.(5) suggests. The dimensionless parameters are Prandtl Pr, modified Rayleigh Ra^* and magnetization numbers γ . The air is presumed as the working fluid in this study, thus the Prandtl number is fixed at 0.71. The modified Rayleigh number is fixed at 10^3 and its definition is as follows.

$$Ra^* = g\beta q\ell^4 / \lambda D\nu \quad (12)$$

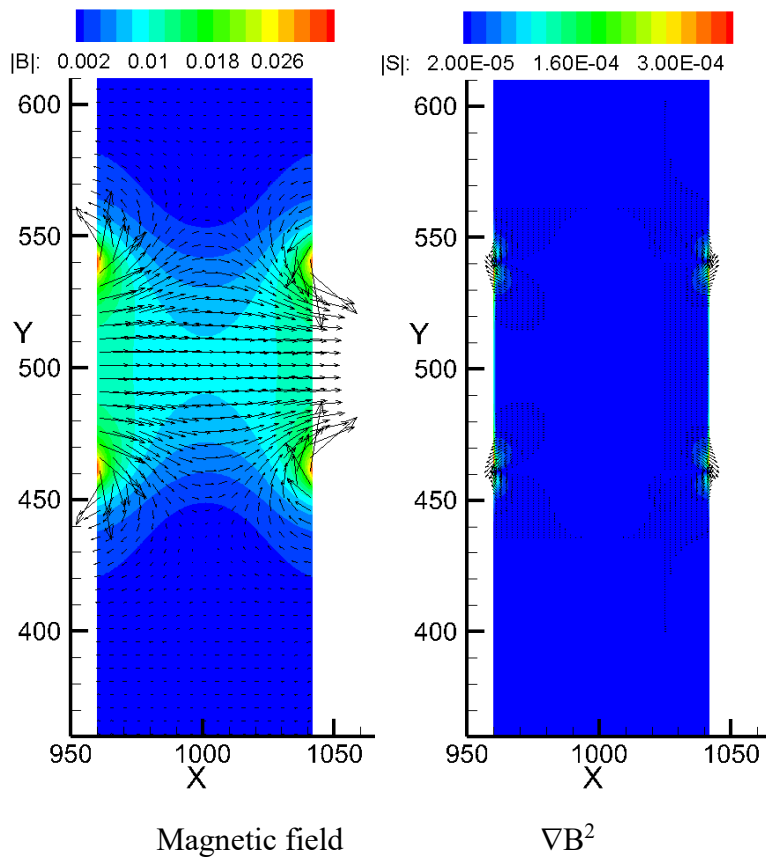
The dimensionless magnetic induction γ defined as follows,

$$\gamma = \chi_m b^2 / (\rho g \mu_m \ell) \quad (13)$$

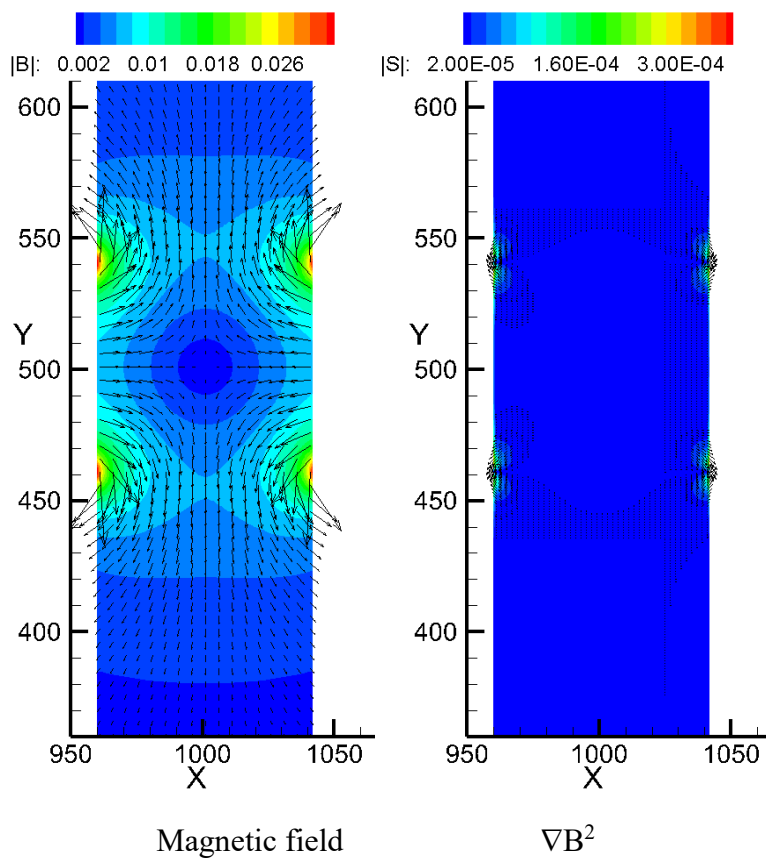
The magnetothermal force with isothermal contours are shown in Fig. 4 at $\gamma = 10^4$. The applied magnetic field is identical to Fig.3. As expected, the force becomes remarkable where the ∇B^2 becomes large. In other words, the magnetothermal force is effective near the electric wires. The distribution of the magnetothermal force is also similar each other. For both cases, the force is induced along the magnet area, and is directed to the center. At the upper and lower magnet edges, the magnetothermal force becomes large. Since the distribution of ∇B^2 is similar in both cases, the magnetothermal force distribution is almost same except in the vicinity of the electric wire location.

Heat and fluid flow The isothermal contours and velocity profiles are shown in Fig.5. Since the profile of the magnetothermal force is similar in both cases, the velocity and temperature profiles are similar. It is found that, the thermal boundary layer is interrupted at the wire elevation. A small vortex can be observed at this location. The buoyant flow goes up detouring this vortex region. This occurs four locations corresponding to the wire location. However, the effect is remarkable at the upper wires since the force becomes stronger by higher temperature. Additionally, this vortex and detouring flow is similar to the forced convection inside the pipe under the one-turn coil magnetic field [12].

When the magnetic field becomes stronger, the vortex becomes large. Fig.6 shows the results at $\gamma=5 \times 10^4$. It can be concluded that, when the electric wire is employed to induce the magnetic field, the effect of the magnetic field on the natural convection is comparable regardless of the direction of the magnetic field.

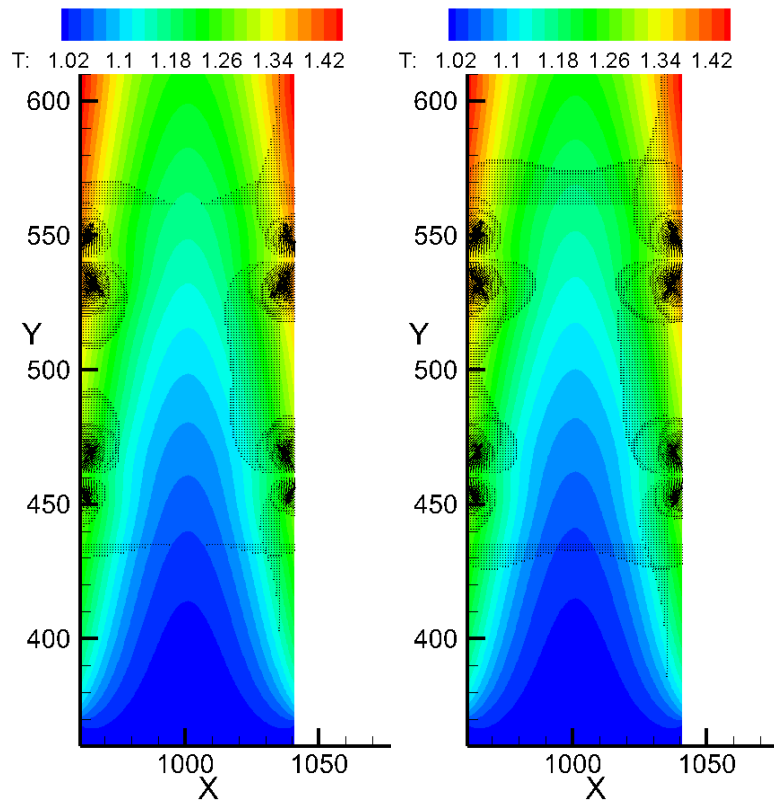


(a) uniform magnetic field



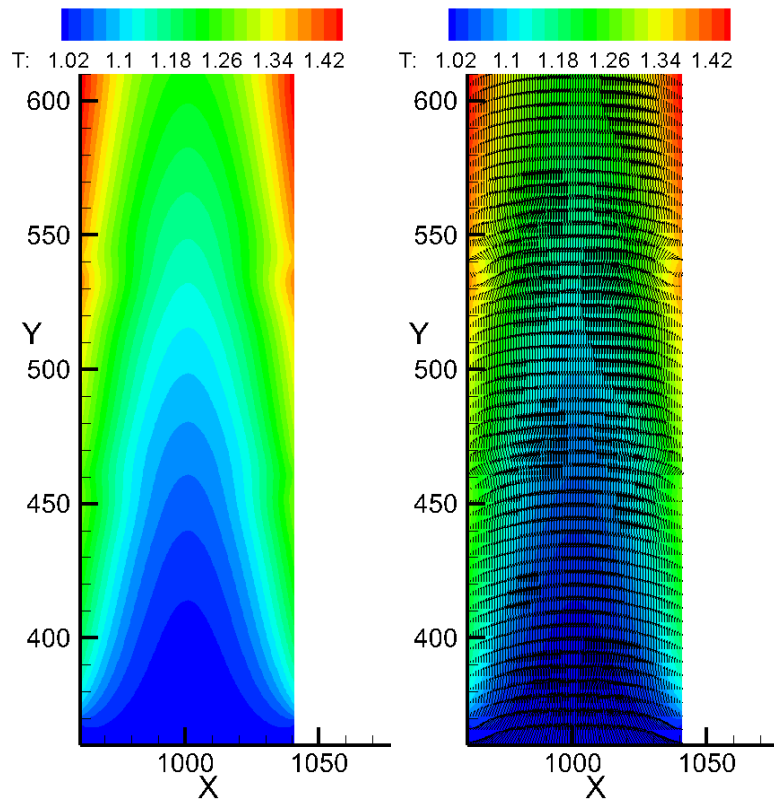
(b) cusp-shape magnetic field

Fig. 3 Magnetic field and ∇B^2

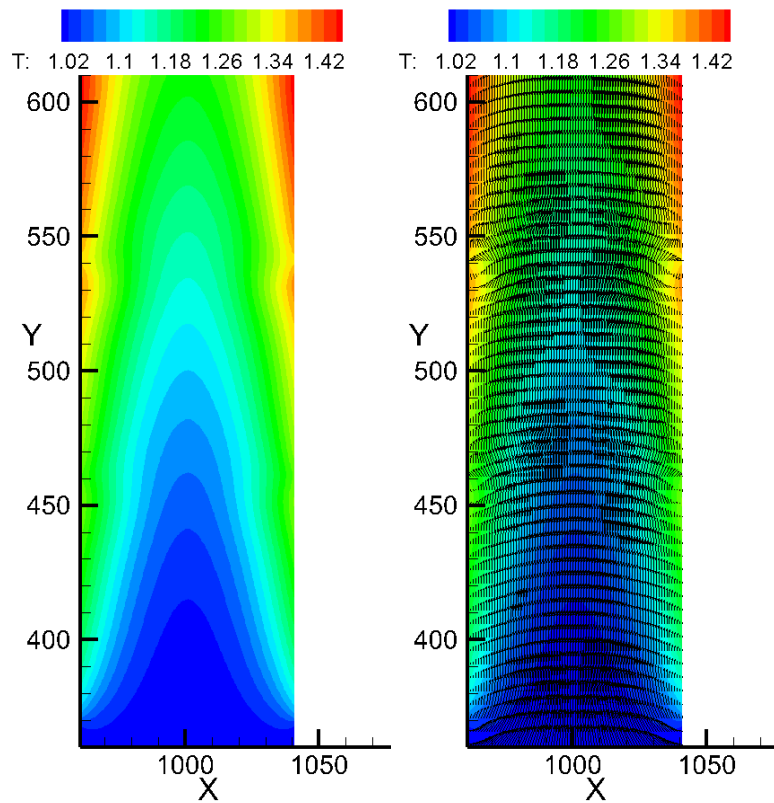


(a) uniform magnetic field (b) cusp-shape magnetic field

Fig. 4 Magnetothermal force with isotherms at $Pr=0.71$, $Ra^*=10^3$, and $\gamma=10^4$.

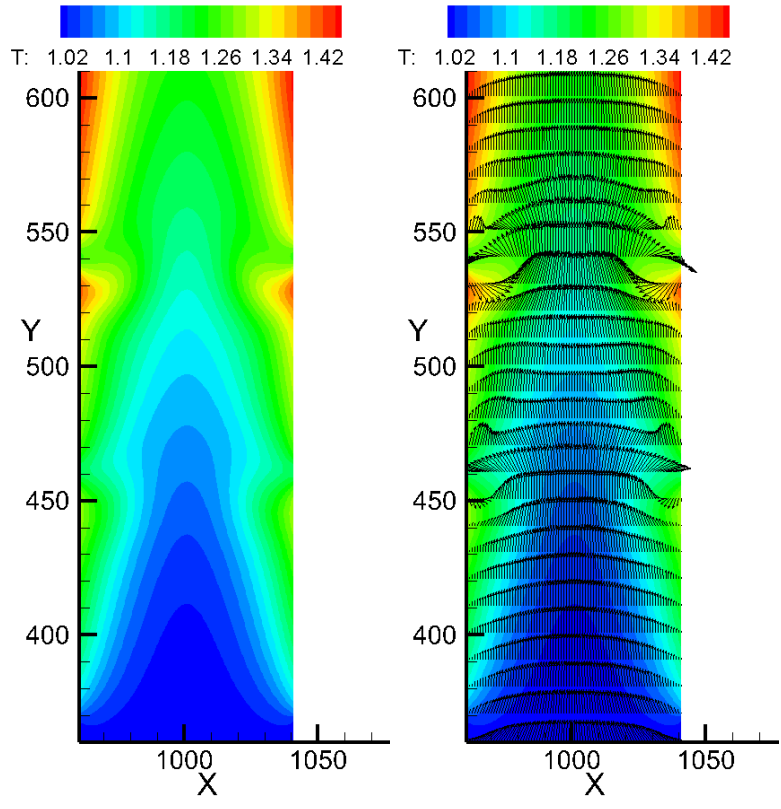


(a) uniform magnetic field

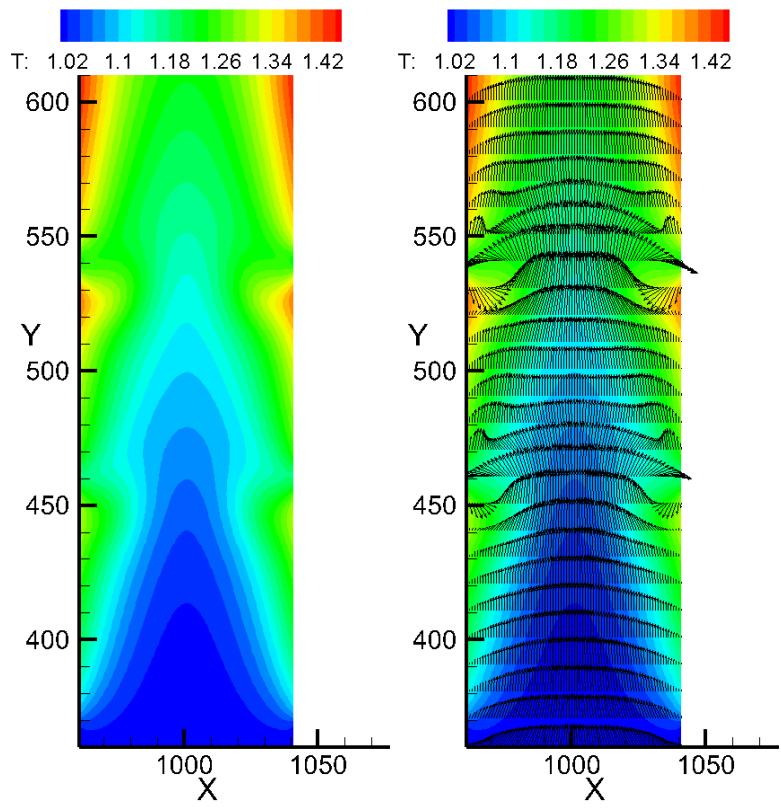


(b) cusp-shape magnetic field

Fig. 5 Isotherms and velocity vectors at $Pr=0.71$, $Ra^*=10^3$, and $\gamma=10^4$.



(a) uniform magnetic field



(b) cusp-shape magnetic field

Fig. 6 Isotherms and velocity vectors at $Pr=0.71$, $Ra^*=10^3$, and $\gamma=5 \times 10^4$.

Local Nusselt Number along the Wall Finally, the effect on the local heat transfer is investigated by the local Nusselt number. Figure 8 shows the local Nusselt number along the heated wall. The definition of the local Nusselt number is as follows,

$$Nu = \frac{ql}{(T_{wall} - T_{ave})} \quad (14)$$

where T_{ave} is local mixed mean temperature.

The heat transfer is suppressed below the wire elevation and it is enhanced above the wire elevation. In cases of weak magnetic induction ($\gamma=10^4$), the effect is small and the enhancement and suppression is in the same magnitude. As the magnetic induction becomes stronger ($\gamma=5 \times 10^4$), the enhancement becomes remarkable. This is due to the enhancement of the vortex near the wall, which facilitates the local convection. As shown in aforementioned sections, the effect has the similar profile regardless of the magnetic direction. Therefore, the magnetic field induced by electric wires has the similar tendency of the effect.

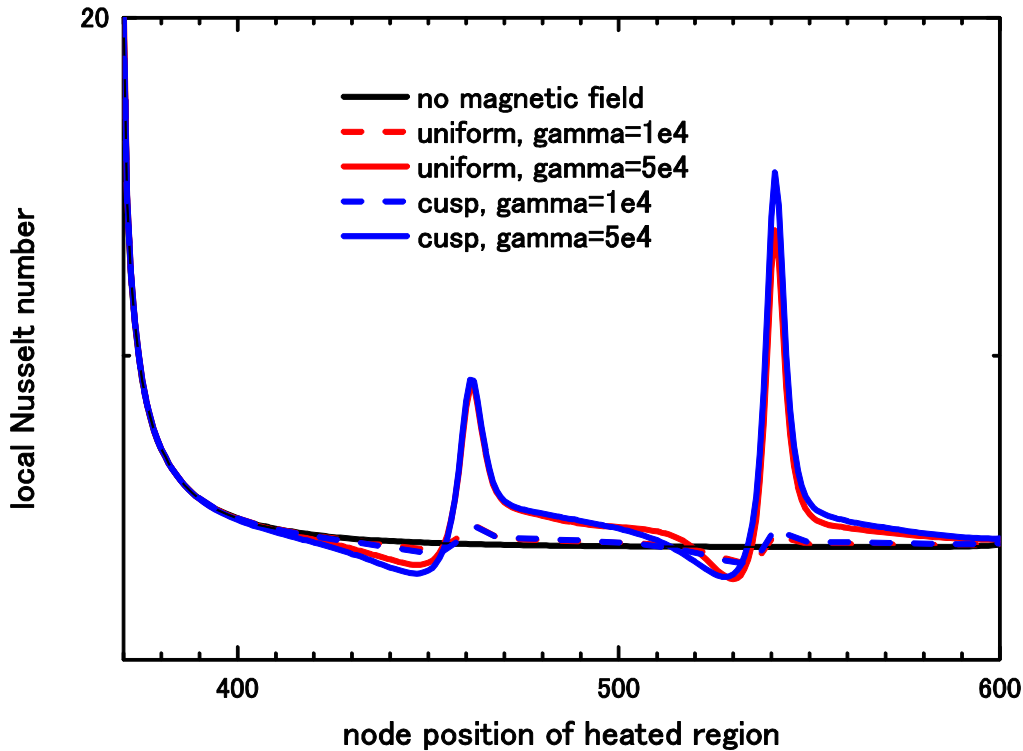


Fig. 7 Local Nusselt number along the heated wall.

CONCLUSION

The magnetothermal convection of air is numerically investigated in the natural convection between parallel plates. The computations are carried out by the lattice Boltzmann method. Firstly, the appropriate relaxation times are obtained by the numerical test in the natural convection inside a square cavity. For the computation of the parallel plates, it is found that the thermal boundary layer is affected at the wire elevation where the magnetic field is induced. The natural convection is suppressed below the wire

elevation whereas it is enhanced above it. This is due to the vortices induced by the magnetothermal force under the buoyancy flow. It is found that, the magnetic field direction is not a dominant factor on these phenomena as far as the magnetic field is induced by electric wires. In other words, the magnetic field in the vicinity of the electric wire is dominant on the heat and fluid flow. These results suggest that the application of the strong magnetic field is effective to enhance the heat transfer of such as the small-sized heat sinks, where the natural convective heat transfer occurs.

ACKNOWLEDGEMENT

This study is partially supported by MEXT, Grant-in-aid for Scientific Research (C) No. 15K05838.

REFERENCES

- [1] Faraday, M.: On the diamagnetic conditions of flame and gases. London, Edinb. Dubl. Phil. Mag. J. Sci. XXXI, third ser. 401–421 (1847)
- [2] Ikezoe, Y., Hirota, N., Nakagawa, J., Kitazawa, K.: Making Water Levitate. *Nature*, 393, 749-750 (1988)
- [3] Wakayama, N.I.: Behavior of Gas Flow under Gradient Magnetic Fields. *J. Appl. Phys.*, 69, 2734-2736 (1991)
- [4] Kitazawa, K., Ikezoe, Y., Uetake, H., Hirota, N.: Magnetic field effects on water, air and powders. *Physica B: Condensed Matter*, 294, 709-714 (2001)
- [5] Maki S., Ataka M., Tagawa T., Ozoe H., Mori W.: Natural Convection of a Paramagnetic Liquid Controlled by Magnetization Force. *AIChE Journal*, 51, 1096-1103 (2005)
- [6] Braithwaite, D., Beaugnon, E., Tournier, R., Magnetically Controlled Convection in a Paramagnetic Fluid, *Nature*, 354, no. 6349, 134–136 (1991)
- [7] Kaneda M., Noda, R., Tagawa, T., Ozoe, H., Lu, S-S, Hua, B.: Effect of inclination on the convection of air in a cubic enclosure under both magnetic and gravitational fields with flow visualization, *J. Chemical Engineering of Japan*, 37,2,338-346(2004)
- [8] Wrobel W.A., Fornalik-Wajs E. and Szmyd J.S.: Analysis of the Influence of a Strong Magnetic Field Gradient on Convection Process of Paramagnetic Fluid in the Annulus between Horizontal Concentric Cylinders, *J. Phys: Conf. Ser.*, 395, 012124 (2012)
- [9] Bednarz T., Tagawa T., Kaneda M., Ozoe H. and Szmyd J.S.: Magnetic and Gravitational Convection of Air with a Coil Inclined around the X Axis, *Num. Heat Trans.*, 46, 99-113 (2004)
- [10] Uetake, H., Hirota, N., Nakagawa, J., Ikezoe, Y., Kitazawa, K.: Thermal Convection Control by Gradient Magnetic Field”. *J. Appl. Phys.*, 87(9), 6310-6312 (2000)
- [11] Uetake, H., Nakagawa, J., Horota, N., & Kitazawa, K.: Nonmechanical magnetothermal wind blower by a superconducting magnet. *Journal of applied physics*, 85(8), 5735-5737 (1999)
- [12] Kaneda, M., Tsuji, A., Ooka, H., & Suga, K.: Heat transfer enhancement by external magnetic field for paramagnetic laminar pipe flow. *International Journal of Heat and Mass Transfer*, 90, 388-395 (2015)
- [13] Akamatsu, M., & Higano, M.: Magnetothermal wind visualized by numerical computation. *Journal of visualization*, 10(3), 261-270 (2007)
- [14] Kaneda, M., Suga, K.: Magnetothermal force on heated or cooled pipe flow. *International Journal of Heat and Fluid Flow*, 69, 1-8 (2018)
- [15] He X., Chen S. and Doolen G.D.: A Novel Thermal Model for the Lattice Boltzmann Method in Incompressible Limit”. *J. Comput. Phys.*, 146, 282-300 (1998)
- [16] Kaneda M., Kano H. and Suga K.: Development of Magneto-Thermal Lattice Boltzmann Heat and Fluid Flow Simulation. *Heat Mass Trans.*, 51, 1263-1275 (2015)

[17] Hortmann, M., Perić, M., & Scheuerer, G.: Finite volume multigrid prediction of laminar natural convection: Bench-mark solutions. *International journal for numerical methods in fluids*, 11(2), 189-207 (1990).

[18] de Vahl Davis G.: Natural Convection of Air in a Square Cavity: A Benchmark Numerical Solution. *Int. J. Numer. Meths. Fluids*, 3, 249–264 (1983).